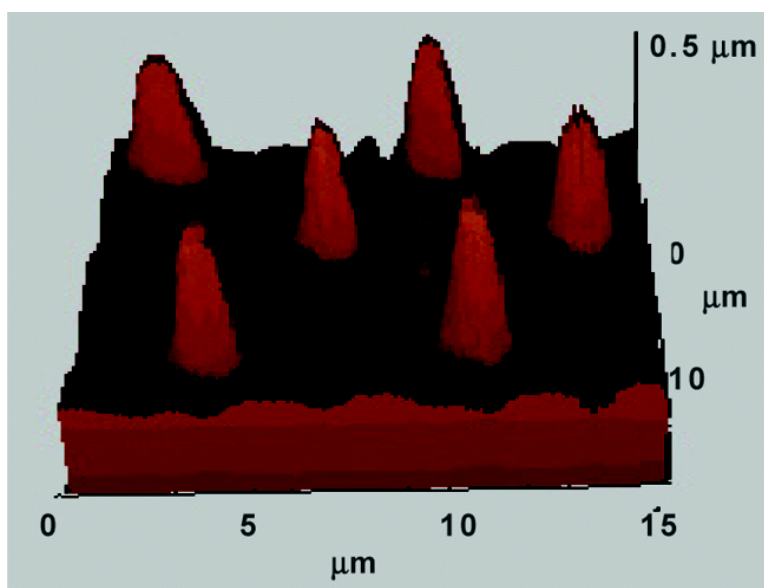


## Surface-Localized Release of Nitric Oxide via Sol–Gel Chemistry

Mary E. Robbins, and Mark H. Schoenfisch

*J. Am. Chem. Soc.*, **2003**, 125 (20), 6068-6069 • DOI: 10.1021/ja034019o • Publication Date (Web): 26 April 2003

Downloaded from <http://pubs.acs.org> on March 26, 2009



### More About This Article

Additional resources and features associated with this article are available within the HTML version:

- Supporting Information
- Links to the 1 articles that cite this article, as of the time of this article download
- Access to high resolution figures
- Links to articles and content related to this article
- Copyright permission to reproduce figures and/or text from this article

[View the Full Text HTML](#)

## Surface-Localized Release of Nitric Oxide via Sol–Gel Chemistry

Mary E. Robbins and Mark H. Schoenfish\*

Department of Chemistry, University of North Carolina at Chapel Hill, Chapel Hill, North Carolina 27599

Received January 2, 2003; E-mail: schoenfi@email.unc.edu

A significant challenge that has prevented the development of viable intravascular sensors is biofouling of the blood-contacting interface due to protein deposition, platelet adhesion/activation, and surface-induced thrombosis.<sup>1–3</sup> Strategies reported for improving implant–blood compatibility include the use of more blood compatible polymers<sup>4</sup> (e.g., silicone rubbers, polyurethane), specific surface modifications via albumin, heparin, or plasma coatings, and endothelial cell seeding.<sup>5,6</sup> To date, these approaches have been met with only limited success *in vivo*; platelet adhesion and coagulation events still dominate the interfacial chemistry that occurs between a polymer-based medical device and blood.<sup>7,8</sup> A promising solution to these blood compatibility problems involves the use of polymers that controllably release nitric oxide (NO). NO is naturally produced by endothelial cells where it functions to promote vasodilation of the surrounding blood vessels and regulate platelet adhesion/activation at the blood–endothelium interface.<sup>9</sup> Polymers capable of mimicking the vascular endothelium have been synthesized by incorporating diazeniumdiolate NO donor molecules into polymeric matrixes. Such coatings have successfully been applied to a wide range of biomedical implants including vascular grafts<sup>10</sup> and gas/electrolyte sensors.<sup>11</sup> Although improved blood compatibility has been reported for oxygen-catheter sensors coated with thin NO-releasing polymers for up to 24 h,<sup>12</sup> thicker films necessary for devices requiring longer NO release (e.g., subcutaneous sensors) were found to inhibit analyte diffusion, resulting in poor analytical sensitivity.<sup>13</sup> Herein, we employ micropatterning methods to selectively modify surfaces with arrays of NO-releasing sol–gels such that the majority of the underlying substrate remains unmodified while the overall interface is uniquely resistant to platelet adhesion.

We have previously reported on the use of aminosilane-based sol–gels for the localized release of NO.<sup>14</sup> Sol–gel chemistry has proven to be an effective strategy for generating NO in a controllable manner. In this report, the ability of sol–gel films and micropatterns to reduce *in vitro* platelet adhesion is investigated.

Sol–gel materials were synthesized by combining methyltrimethoxysilane (MTMOS), ethanol, water, and (aminoethylamino-methyl)phenethyltrimethoxysilane (AEMP3) and sonicating for 5 min. Due to the low viscosity of the sol solution, which is an attractive feature for patterning applications, 20% AEMP3/80% MTMOS sol–gels were employed for this study. Sol–gel films were cast onto ethanol-cleaned glass slides (ca. 2 cm<sup>2</sup>) using 10  $\mu$ L of sol solution. The sol–gel films were then cured, dried, and aged at room temperature under atmospheric conditions for 24 h. Sol–gel microarrays were prepared by either an applied pressure<sup>15</sup> or capillary flow<sup>16</sup> method using elastomeric poly(dimethylsiloxane) (PDMS) templates made from silicon (Si) masters. To fabricate microarrays using applied pressure, the sol solution was placed directly onto a substrate and covered with a PDMS template. Pressure was applied using a microbar clamp to allow for contact between the template and underlying substrate. Micropatterning by capillary flow was achieved by placing a PDMS template consisting

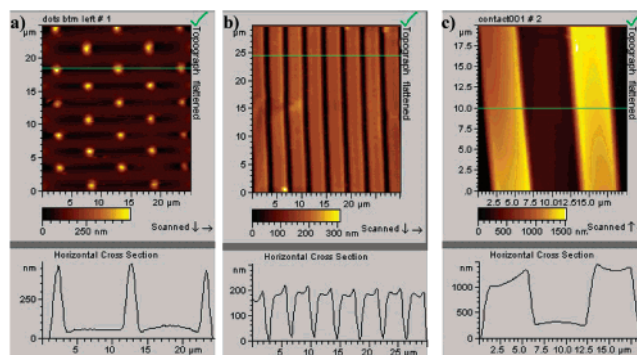


**Figure 1.** Contact mode AFM images of 20% AEMP3/80% MTMOS sol–gel micropatterns on glass. Patterns (a) (1  $\mu$ m dots  $\times$  10  $\mu$ m spaces) and (b) (3  $\mu$ m lines  $\times$  1  $\mu$ m spaces) were prepared by applied pressure. Pattern (c) (5  $\mu$ m lines  $\times$  7  $\mu$ m spaces) was prepared by capillary flow.

of an array of straight channels in direct contact with a glass substrate. Sol solution placed at one end of the array was drawn into the microchannels via capillary action.<sup>16</sup> For both patterning methods, the template was removed after curing/drying for 24 h. Sol–gel microarrays were characterized using atomic force microscopy (AFM). Representative AFM images of AEMP3/MTMOS micropatterns are shown in Figure 1. Feature dimensions were determined using the horizontal line scan that accompanies each image. Notably, a variety of sol–gel microarrays can be formed using applied pressure and capillary flow patterning methods (Figure 1).

The amine groups in the sol–gel patterns were then converted to diazeniumdiolate NO donors<sup>17</sup> via exposure to 5 atm of NO for 72 h. Diazeniumdiolate formation was confirmed by the appearance of a characteristic band at 250 nm in the solid-state UV–vis absorbance spectra of analogous films cast on quartz slides.<sup>14</sup> The ability of micropatterned sol–gel lines to withstand these conditions and those necessary to initiate NO release (solution immersion<sup>14</sup>) was also assessed using AFM. Micropatterns were imaged before and after exposure to 5 atm of NO for 72 h. Changes in the sol–gel microarray geometry were not observed following high-pressure NO gas exposure. AFM images at distinct intervals after immersion in Tyrode’s buffer (pH 7.35) at 37  $^{\circ}$ C indicate that the stability of the sol–gel patterns was maintained in aqueous solution for up to 7 d (data not shown). Sol–gel micropattern stability was also evaluated by measuring the concentration of Si in Tyrode’s buffer soak solutions as a function of immersion time using direct current plasma (DCP) emission spectroscopy. The concentration of Si in soak solutions for AEMP3/MTMOS sol–gel micropatterns was below the limit of detection (<0.5 ppm) for up to 24 h immersion. The rate of NO release in Tyrode’s buffer at 37  $^{\circ}$ C was measured using a NO chemiluminescence analyzer and found to be steady for at least 1 h and continuous for up to 24 h (Supporting Information). Of note, we have previously shown that both the rate and duration of NO release from sol–gels may be increased by varying the percent (v/v) and/or type of silicon alkoxides.<sup>14</sup> Indeed,

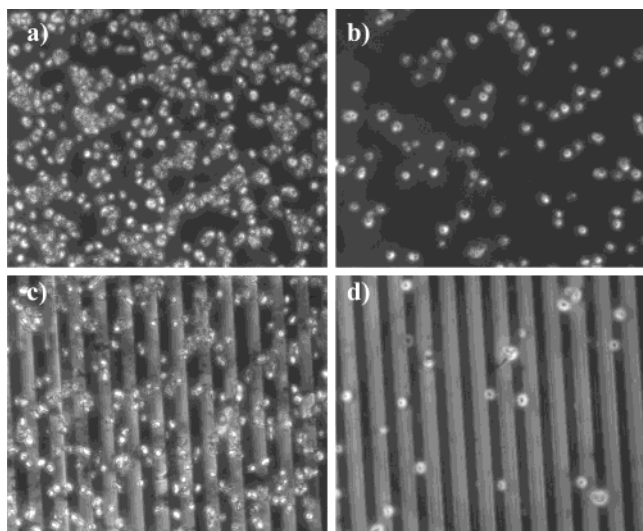


**Figure 2.** Phase contrast microscopy images ( $167 \times 167 \mu\text{m}^2$ ) of porcine platelet adhesion to 20% AEMP3/80% MTMOS (a) control film, (b) NO-releasing film, (c) control micropattern, (d) NO-releasing micropattern.

**Table 1.** Porcine Platelet Adhesion to 20% AEMP3/80% MTMOS Sol-Gel Modified Substrates

	NO flux ( $\text{pmol}/\text{cm}^2\cdot\text{s}$ )	platelet coverage <sup>a</sup> (%)		ANOVA $\rho$ value
		control	NO-releasing	
film	$2.3 \pm 0.4$	$120 \pm 47$	$28 \pm 18$	$3.6 \times 10^{-14}$
pattern	$2.2 \pm 0.4$	$75 \pm 24$	$19 \pm 12$	$1.4 \times 10^{-13}$
$\rho$ value		$2.3 \times 10^{-3}$	0.02	

<sup>a</sup> Platelet coverage measured by percent opaqueness in a  $167 \times 167 \mu\text{m}^2$  image area relative to glass control. Averages and standard deviations determined from 10 images from 3 independent surfaces ( $n = 30$ ).

sol-gel coatings that controllably release NO for up to 7 d have been prepared (data not shown).

Because a material's blood compatibility is directly related to its ability to prevent platelet adhesion, *in vitro* platelet adhesion studies using platelet-rich porcine plasma<sup>2</sup> were used to characterize the blood compatibility of NO-releasing AEMP3/MTMOS sol-gel films and microarrays. As shown in the phase contrast microscopy images in Figure 2, both control sol-gel films (Figure 2a) and sol-gel micropatterns ( $5 \mu\text{m}$  lines,  $7 \mu\text{m}$  spaces) were characterized by dense platelet adhesion (Figure 2c). In contrast, the coverage of platelets on films that release NO (Figure 2b) was significantly reduced, suggesting that NO release is effective at inhibiting platelet adhesion. A statistically significant ( $\rho \ll 0.001$ ) reduction in platelet adhesion to NO-releasing films relative to controls is noted (Table 1). These results are consistent with previous *in vitro* and *in vivo* platelet adhesion studies demonstrating increased blood compatibility for polymers that release NO.<sup>11,12,18,19</sup>

NO-releasing sol-gel micropatterns (Figure 2d) exhibit a comparable reduction in platelet adhesion when compared to control sol-gel films (Figure 2a) and micropatterns (Figure 2c). These results demonstrate that the localized concentration of NO between sol-gel micropattern lines ( $5 \mu\text{m}$  lines,  $7 \mu\text{m}$  spaces) is above the critical threshold necessary to inhibit platelet adhesion to unmodified regions of the substrate. Thus, the ability of micropatterned NO-releasing surfaces to resist platelet adhesion via surface localized

NO release may be an effective strategy for achieving enhanced sensor biocompatibility without modifying an entire surface and potentially compromising analytical sensitivity.

The measured NO surface flux from AEMP3/MTMOS sol-gel materials was found to be on the order of the NO surface flux from stimulated endothelial cells ( $\sim 6 \text{ pmol}/\text{cm}^2\cdot\text{s}$ ).<sup>20</sup> The total amount of NO released from these materials is, however, still lower than the amount of NO produced daily by the human endothelium ( $\geq 1 \text{ mmol}$ ).<sup>21</sup> Preliminary results indicate that the overall NO release from a substrate may be tuned by varying micropattern dimensions and geometry (Supporting Information). Studies are underway to determine the optimum NO flux, micropattern geometry, and sol-gel composition that most effectively reduces platelet adhesion while maximizing the substrate surface area that remains unmodified.

**Acknowledgment.** We gratefully acknowledge Prof. Thomas Fischer for helpful discussions, and the Francis Owen Blood Research Laboratory for providing blood samples. This research was supported in part by the National Institutes of Health (NIH EB000708). M.N. acknowledges a National Science Foundation Graduate Research Fellowship.

**Supporting Information Available:** Details on the synthesis of AEMP3/MTMOS sol-gels, micropatterning procedures, AFM stability studies and the procedure for porcine platelet adhesion studies (PDF). This material is provided free of charge via the Internet at <http://pubs.acs.org>.

## References

- (1) Cazenave, J.-P.; Mulvihill, J. In *The Role of Platelets in Blood-Biomaterial Interactions*; Missirlis, Y. F., Wautier, J.-L., Eds.; Kluwer: Dordrecht, 1993; pp 69–80.
- (2) Cazenave, J.-P. In *Blood-Surface Interactions: Biological Principles Underlying Haemocompatibility with Artificial Materials*; Cazenave, J.-P., Davies, J. A., Kazatchkine, M. D., Van Aken, W. G., Eds.; Elsevier: Amsterdam, 1986; pp 89–105.
- (3) Lane, D. A.; Bowry, S. K. *Nephrol. Dial. Transplant* **1994**, *9*, 18–28.
- (4) Yoda, R. *J. Biomat. Sci., Polym. Ed.* **1998**, *9*, 561–626.
- (5) Walpoth, B. H.; Rogulenko, R.; Tikhvinskaia, E.; Gogolewski, S.; Schaffner, T.; Hess, O. M. *Circulation* **1998**, *98*, 319–323.
- (6) Pasic, M.; Muller-Glauser, W.; von Segesser, L.; Odermatt, B.; Lachat, M.; Turina, M. *Euro. J. Cardio-Thor. Surg.* **1996**, *10*, 372–379.
- (7) Anderson, J. M.; Kottke-Marchant, K. *Crit. Rev. Biocompat.* **1985**, *1*, 111–204.
- (8) Banerjee, R.; Nageswari, K.; Puniyani, R. R. *J. Biomat. Appl.* **1997**, *12*, 57–76.
- (9) Radomski, M. W.; Rees, D. D.; Dutra, A.; Moncada, S. *Br. J. Pharmacol.* **1992**, *107*, 745–749.
- (10) Hanson, S. R.; Hutsell, T. C.; Keefer, L. K.; Mooradian, D. L.; Smith, D. J. *Adv. Pharmacol. (San Diego)* **1995**, *6*, 383–398.
- (11) Espadas-Torre, C.; Oklejas, V.; Mowery, K. A.; Meyerhoff, M. E. *J. Am. Chem. Soc.* **1997**, *119*, 2321–2322.
- (12) Schoenfish, M. H.; Mowery, K. A.; Rader, M. V.; Baliga, N.; Wahr, J. A.; Meyerhoff, M. E. *Anal. Chem.* **2000**, *72*, 1119–1126.
- (13) Shin, J. H.; Marxer, S. M.; Schoenfish, M. H. *Society for Biomaterials 28th Annual Meeting Transactions*, 2002; p 371.
- (14) Nablo, B. J.; Chen, T.-Y.; Schoenfish, M. H. *J. Am. Chem. Soc.* **2001**, *123*, 9712–9713.
- (15) Yang, P.; Deng, T.; Zhao, D.; Feng, P.; Pine, D.; Chmelka, B. F.; Whitesides, G. M.; Stucky, G. D. *Science* **1998**, *282*, 2244–2247.
- (16) Kim, Y.-D.; Park, C. B.; Clark, D. S. *Biotechnol. Bioeng.* **2001**, *73*, 331–337.
- (17) Hrabie, J. A.; Klose, J. R.; Wink, D. A.; Keefer, L. K. *J. Org. Chem.* **1993**, *58*, 1472–1476.
- (18) Smith, D. J.; Chakravarthy, D.; Pulfer, S.; Simmons, M. L.; Hrabie, J. A.; Citro, M. L. *J. Med. Chem.* **1996**, *39*, 1148–1156.
- (19) Mowery, K. A.; Schoenfish, M. H.; Saavedra, J. E.; Keefer, L. K.; Meyerhoff, M. E. *Biomaterials* **2000**, *21*, 9–21.
- (20) Radomski, M. W.; Palmer, R. M.; Moncada, S. *Biochem. Biophys. Res. Commun.* **1987**, *148*, 1482–1489.
- (21) Keefer, L. K.; Anderson, L. M.; Diwan, B. A.; Driver, C. L. *Methods (San Diego)* **1995**, *7*, 121–130.

JA0340190